

Synthesis and characterization of Fe-Doped CdO binary system

Hakan ÇOLAK^{a,*}, Orhan TÜRKÖĞLU^b

^aÇankırı Karatekin University, Faculty of Science, Department of Chemistry, Ballica Campus, 18200, Çankırı, Turkey

^bErciyes University, Faculty of Science, Department of Chemistry, 38039, Kayseri, Turkey

This paper reports the synthesis, crystal structure and electrical conductivity properties of Fe-doped CdO powders. Monophase samples, which were indexed as cubic structure in the Fe-CdO system, were determined by X-ray diffraction. The limit solubility of Fe ions in the CdO lattice is 2 mol % after heating at 850 °C. The impurity phase was determined as cubic-CdFe₂O₄. The research focused on the single I- phase, which were synthesized at 850 °C because of the limit of the solubility range is widest at this temperature. It was observed that the lattice parameters of the I-phase decreased with Fe doping concentration. The electrical conductivity values of pure CdO (after heating at 850 °C), 0.25 and 2 mol % Fe-doped CdO samples (after heating at 850 °C) at 100 °C were 79, 525 and 1349 Ω⁻¹ · cm⁻¹, and at 850 °C they were 891, 1413 and 3548 Ω⁻¹ · cm⁻¹, respectively. In other words, electrical conductivity increased with Fe doping.

Key words: II-VI semiconductors, Cadmium oxide, Doped cadmium oxide, Four-point probe dc method.

Introduction

Among II-VI compounds, semiconducting cadmium oxide (CdO) is a promising material for future research and has attracted considerable attention because of its suitable physical properties and because it can be used as an alternative material for opto-electronic devices [1]. In particular, CdO is a good material for solar cell applications due to its high electrical conductivity and optical transmittance in the visible region of the solar spectrum [2]. Also, powder and film materials prepared from pure and metal-doped CdO find applications as photodiodes [3], phototransistors [4], photovoltaics [5], transparent electrodes [6], and IR detectors [7]. These applications are based on its specific optical and electrical properties [8-10].

Generally, CdO powder and film have n-type semiconducting properties with an electrical resistivity of 10⁻²-10⁻⁴ Ω · cm and a band gap in between 2.2-2.7 eV. The preparation procedure and kind of metal dopant used are responsible for these different electrical conductivity values and the variety of optical properties. The intensity of optical and electrical effects of CdO depends on deviations from the ideal CdO stoichiometry (due to cadmium interstitials Cd_(1+X)O or oxygen vacancies CdO_(1-X)), as well as on the size and shape of the particles. The oxide crystallizes in a cubic (sodium chloride) structure with a = 4.695 Å properties [5, 8, 9]. Nonstoichiometric CdO usually exhibits low resistivity due to the native defects of oxygen

vacancies and cadmium interstitials [11]. Hence, low resistivity CdO can be obtained by controlling these native defects. The preparation procedure and the type of dopant used are responsible for variety of the electrical properties [12]. Doping with different elements changes the properties of the CdO samples. It was established experimentally that the doping of CdO with metallic ions of a smaller ionic radius than that of Cd²⁺, such as with Dy [12], Te [13], In [14], Cu [15] improves its electrical conduction. Authors have reported that 2.9 at % Sn-CdO sample results in a low resistivity of 1.59 × 10⁻⁴ Ω · cm, about one-twelfth of the value (2 × 10⁻³ Ω · cm) of the undoped CdO sample [16]. In other studies, it was reported that a 6 wt % In-doped CdO sample had a resistivity of 4.843 × 10⁻⁴ Ω · cm [17] and Ga-doped CdO thin films had a minimum resistivity of 3.7 × 10⁻⁴ Ω · cm [18]. Also, in the literature, one study showed that light doping with Fe improved the dc-conduction parameters of CdO films so that with a 1.3 wt.% Fe doping level, the mobility increased by about 6 times and conductivity by 24 times [19].

Thermal annealing is a widely used method to improve crystal quality and to study structural defects in materials. For semiconductors, thermal annealing is also used to activate dopants. During an annealing process, dislocations and other structural defects will move in the material and adsorption/decomposition will occur on the surface; thus the structure and the stoichiometric ratio of the material will change and this influences the electrical and optical properties of CdO. Structural, electrical and optical properties are vital for semiconductor devices. It is necessary to study how these properties are affected by thermal annealing [20].

*Corresponding author:

Tel : +90-376-218-11-23 (Ext:5044)

Fax: +90-376-218-10-31

E-mail: hakancolak@karatekin.edu.tr

De *et al.* have studied the effect of heat treatment on CdO. In their study, the CdO powder sample was coffee brown in color and black after heat treatment at 400 and 800 °C, respectively, and had an NaCl structure. The black colored polymorph of CdO was about 1000 times more conductive than the yellowish brown CdO sample which had no heat treatment sample [21].

Authors reported that the electrical resistivity (ρ) of CdO samples decreased with increases in temperature because the samples are semiconducting in nature [7]. This reduction in resistivity is due to the removal of defects with temperature [8]. Also, CdO starts to decompose at 900 °C [22].

There are few studies about the Fe-CdO binary system [19, 23] and we believe that Fe doping increased the electrical conductivity of CdO. Therefore, in this work, we synthesized metallic Fe-doped CdO powders at high temperatures by using the solid state reaction method. Then, we studied their crystallographic properties and measured the dc electrical conductivity of the CdO solid solution samples. The solid state reaction was chosen because of its reproducibility, easy control and sufficient products for measurement [24].

Experimental

The Fe-doped CdO powders were synthesised at high temperatures by using a solid state reaction method. At first, we prepared solid mixtures of Fe-CdO (in the range of 0.25-15 mol %) were prepared by mixing and homogenizing them, using stoichiometric amounts of pure CdO and metallic Fe in an agate mortar. As starting materials, commercial pure CdO powders (99.9% Fluka) and metallic iron powders (> 99% Fluka) were used. Pure CdO powders and the powder mixtures were first calcined at 600 and 650 °C for 24 hrs. After grinding and homogenization the pre-annealed mixtures were heat-treated at 700, 750, 800, 850 and 900 °C, respectively. All these heat treatments were made in an air atmosphere for 48 hrs, in alumina crucibles and without any compaction procedure. At the end of each heat treatment procedure, the annealed powders were slowly cooled in the furnace by switching it off (uncontrolled) [25]. Before and after heat treatment each of the samples was ground in an agate mortar to a homogenized powder size.

The samples were then analyzed using X-ray powder diffraction (XRD). The XRD data of the samples were recorded on a computer-interfaced Bruker AXS D8 advanced diffractometer operating in the Bragg-Brentano geometry (Cu $K\alpha$ radiation, graphite monochromator, 40 kV and 40 mA) over a $10^\circ \leq 2\theta \leq 90^\circ$ angular range. Divergence and receiving slits of 1 and 0.1 mm, respectively, were located on the diffractometer. The diffraction patterns were scanned in 0.002° (2θ) steps and the diffracted beams were counted with a NaI (Tl)

scintillation detector [25]. The Diffrac Plus and Win-Index programs were used to obtain information about the crystal structures of the samples. Then, for a comparison with standard data the PDF program (Maint Powder Diffraction Database Manager Software) was used. In all cases, the XRD patterns of the samples, which were obtained as a single phase, could be indexed on the basis of a cubic cell in the Fe-CdO binary system. The single phase was named the I-phase. The other samples, which were out of the solubility range, were heterogeneous solid mixtures of I-phase and the another phase (not indexed with a cubic structure) denoted as II-phase. The morphologies of both annealed (at 850 °C) and non-annealed undoped CdO samples and I-phase samples (after heating at 850 °C) were observed using a scanning electron microscope (SEM, LEO 440) operated at 20 kV. With this aim, before SEM measurement, the I-phase samples in the Fe-CdO binary system were pressed into pellets of 0.1 cm thickness (t) and 1.3 cm in diameter (d) under ~ 4 ton pressure and were calcined at 850 °C for 12 hrs in air. After this heat treatment, XRD measurements showed no phase change in the cubic samples. The average grain sizes of these I-phase samples were calculated by the Image-pro Plus 5.0 program from SEM micrographs. When average grain sizes were calculated, 10 grains were selected at random from the SEM micrographs [26].

The electrical conductivity (σ_{dc}) measurements of the I-phase samples (after heating at 850 °C) were made using the standard four-point probe dc method. The circular samples with a cubic structure, which were mentioned above as the pelleted samples, were used for the electrical conductivity measurements. To reduce contact resistance, fine platinum wires were attached directly to the surface of the samples. The ohmic character of the wire contacts was checked prior to each measurement. The contacts were positioned symmetrically with respect to the centre of the circular pellet and the contact separations (s) were 0.2 cm. The conductivity measurements were made at temperatures between 100 and 850 °C for I-phase samples synthesized at 850 °C. The increase in furnace temperature was initially in 100 °C steps in an air atmosphere. During the measurements, the sample temperature was determined by a thermocouple located 5 mm away from the sample. This thermocouple had a cold (0 °C junction). All experimental data were made by a Keithley 2400 sourcemeter and a Keithley 2700 electrometer which were controlled by a computer [25].

Results and Discussion

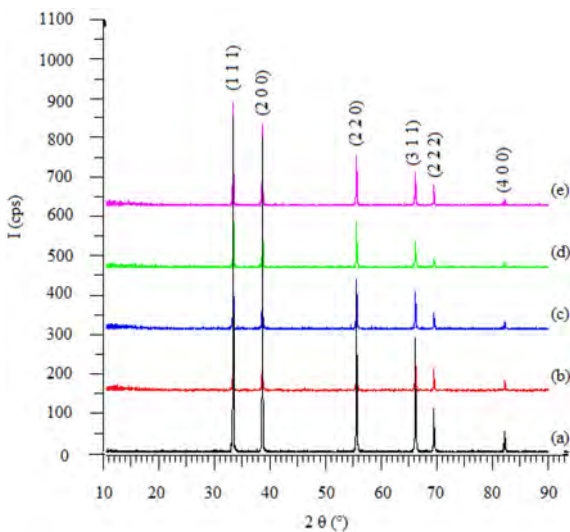
XRD Studies

To investigate the solubility of Fe ions in the CdO crystals, the synthesized different compositions of the Fe-doped CdO binary system were anneal at varying

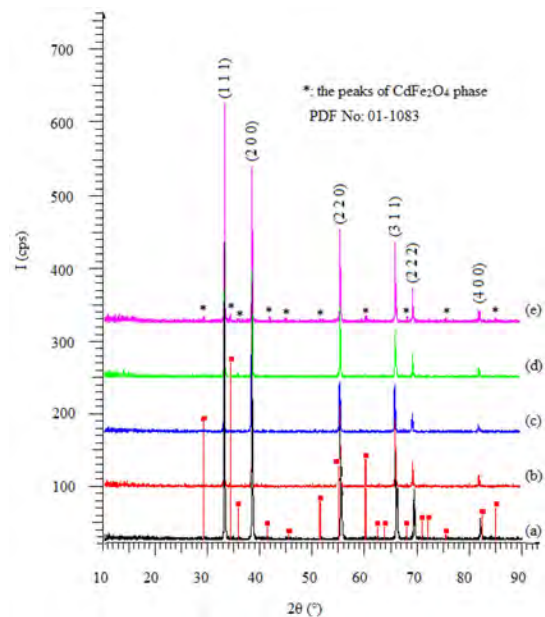
Table 1. Observed phases in the binary system of Fe-doped CdO (in the range of 0.25-15 mol %).

Temp. (°C)	x (Fe addition) / mol %																	
	0.25	0.50	0.75	1	2	3	4	5	6	7	8	9	10	11	12	13	14	15
700	I	I	I	I + II														
750	I	I	I	I	I + II													
800	I	I	I	I	I + II													
850	I	I	I	I	I	I + II												
900	*	*	*	*	*	*	*	*	*	*	*	*	*	*	*	*	*	*

I: Fe-doped CdO (cubic), II: cubic- CdFe_2O_4 , I + II: heterogeneous solid mixtures.
 *: decomposition of Fe-CdO samples.

**Fig. 1.** XRD patterns of Fe-doped CdO (after heating at 850 °C): (a) undoped CdO and (b) 0.25, (c) 0.50, (d) 1, (e) 2 mol %.

temperatures. At first, pure CdO that one of the our starting materials and solid mixtures of Fe-CdO were coffee brown coloured but they were black coloured after first calcined 600, 650 °C and at further heat treatments at 700, 750, 800, 850 and 900 °C. We think that this condition was due to the color centers in the crystal lattice of CdO. The XRD diffraction patterns of the synthesized samples without and with different amounts of Fe in Fe-CdO system (undoped CdO at 850 °C and 0.25, 0.50, 1 and 2 mol % after heating at 850 °C) are shown in Fig. 1. In this figure, all of the XRD patterns show typical peak patterns, which can be indexed as the cubic CdO structure. The diffraction pattern without Fe can be identified as a cubic CdO structure. After the partial substitution of Cd ions by Fe ions, the diffraction pattern (in the range of 0.25-2 mol %, after heating at 850 °C) shows the same peaks, which indicates that the cubic structure is not disturbed by Fe substitution. The XRD patterns of the other single I-phase samples, which were synthesized at other temperatures, were quite similar to the patterns of the I-phase samples given in Fig. 1. No additional peaks are observed in this range due to the absence of any impurity. However, when the doping concentration

**Fig. 2.** XRD patterns of undoped and Fe-doped CdO samples (after heating at 850 °C): (a) pure CdO, (b) 3, (c) 5, (d) 7, (e) 10 mol %.

of Fe was increased above 2 mol % (at 850 °C), the CdFe_2O_4 (PDF no: 01-1083) peaks could be clearly seen in the XRD pattern which is shown in Fig. 2 [27]. After heating at 850 °C, the XRD measurements revealed that doping with more than 2 mol % Fe caused the coexistence of the I and II phase. No indication of Fe metal impurities was observed in our samples. In the Fe-doped CdO binary system, the observed single phases and heterogeneous solid mixtures depend on the reaction temperature and amounts of Fe doping, as presented in Table 1. It can be seen from this table that the widest range of solubility in the CdO lattice for Fe ions is found after heating at 850 °C, and at this temperature the solubility limit is 2 mol %. At lower temperatures the solubility range is lower than observed at 850 °C. The low solubility of Fe ions may be explained by the heterovalence of the Fe ions (2+ and 3+) in the CdO host lattice. The mobility of Fe ions, which diffuse in the CdO octahedral sites [28,29], increase with temperature. The heat treatment temperature was found

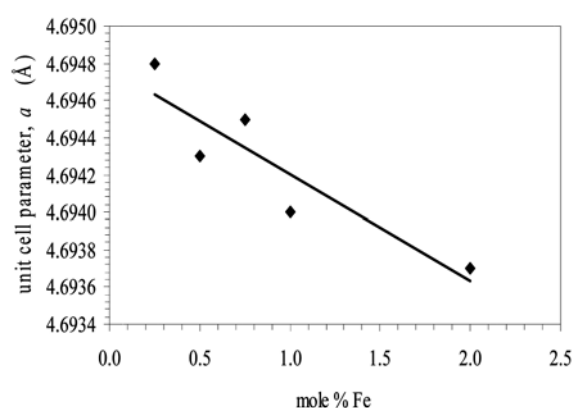
Table 2. 2θ , d and I/I_0 values for the pure CdO and 2 mol % Fe-doped CdO samples (after heating at 850 °C).

No	h k l	pure CdO			2 mol % Fe-CdO		
		2θ (°)	d [Å]	I/I_0	2θ (°)	d [Å]	I/I_0
1	1 1 1	33.041	2.7089	100	33.045	2.7086	100
2	2 0 0	38.339	2.3459	84.9	38.359	2.3455	72.4
3	2 2 0	55.323	1.6592	39.1	55.346	1.6586	69.8
4	3 1 1	65.964	1.4151	34.1	65.986	1.4146	39.1
5	2 2 2	69.303	1.3548	15.6	69.335	1.3542	13
6	4 0 0	82.065	1.1734	6.4	82.091	1.1732	9.1

to have an effect on the solubility of Fe ions in CdO. Generally, as the sintering temperature increased, the solubility limit increased because of an endothermic reaction [30, 31]. We observed the solid mixture of the Fe-CdO samples started to decompose after heat treatment at 900 °C. In the XRD patterns of the samples after heating at 900 °C showed an increase in the intensity of the background lines and width of peaks. So, according to these results, we observed the transformation of cubic structure to an amorphous structure.

In addition, both ionic radii and valence state are important factors in determining the solubility of the dopants [32]. Focused on single I- phase, CdO samples were synthesized at 850 °C because of the widest range of the solubility at this temperature. The other I- phase samples synthesized at temperatures lower than 850 °C, and the multiphase samples (I + II) were excluded from this study. Also, the lattice spacing d , I/I_0 ratio, angle of diffraction 2θ in the phases identified along with the (hkl) planes of the pure CdO and 2 mol % Fe-doped CdO samples (after heating at 850 °C) are given in Table 2. It is shown in this table that there is a slight shift in the Bragg angle of the peaks towards higher values with Fe doping concentration. This slight shift in the peaks resulted from the created structural strain accompanied with Fe doping, which has a slightly lower ionic radius (for Fe^{2+} : 0.77 Å and Fe^{3+} : 0.69 Å) than that of the Cd^{2+} ion (0.95 Å) [33].

The lattice constants of pure CdO (starting material) ranged from 4.6740 to 4.6900 Å (from room temperature to 850 °C), whereas the values of I- phase CdO samples (850 °C) ranged from 4.6948 to 4.6937 Å. Our results are very close to those of other reports [19, 34]. The deviation from that of the ideal cubic crystal is probably due to lattice stability and ionicity [35]. For pure CdO, the unit cell parameter slightly increased with the increase in heat treatment temperatures, and in our opinion this was due to crystal strain. Figure 3 shows the dependence of the lattice parameter a on the mol fraction of Fe. The calculated unit cell parameters of the single I- phase samples slightly decrease with Fe doping concentration. This indicates that Fe ions are incorporated in the crystal

**Fig. 3.** Change in the unit cell parameters of I- phase CdO samples after heating at 850 °C.

structure of CdO since the lattice parameters display systematic variation. The decrease in lattice parameters is in good agreement with effective ionic radii considerations. However, the ionic radius (six-coordinated) of the Fe^{2+} ion is 0.77 Å and that of the Fe^{3+} ion is 0.69 Å while the ionic radius of the Cd^{2+} is 0.95 Å [33]. Therefore, the decrease in the lattice parameter can be explained by the ionic radii difference. The lattice parameters of a semiconductor usually depend on the following factors: (i) free electron concentration acting via the deformation potential of a conduction-band minimum occupied by these electrons, (ii) concentration of foreign atoms and defects and the difference in ionic radii with respect to the substituted matrix ion, (iii) external strains for example, those induced by the substrate, and (iv) temperature [35].

Surface morphological studies

Fig. 4 shows the SEM micrographs of both annealed (850 °C) and non-annealed undoped CdO and I- phase CdO samples (after heating at 850 °C). In the SEM micrographs of undoped CdO samples there is a homogeneous grain distribution. For the I- phase samples, it is shown the homogeneous grain distribution is eliminated and agglomeration is increased by the increase in the Fe doping concentration. The average grain sizes were not calculated due to agglomeration but from the scale bar on the SEM micrographs it is estimated they are about 10 μm. Also, some pores can be noticed from the SEM micrographs.

Electrical conductivity measurements

The total electrical conductivity is calculated using the following equation:

$$\sigma_T = \frac{I}{V} G^{-1} \quad (1)$$

where G is the geometric resistivity correction factor. In the calculation of electrical conductivity there is a functional relation between sample geometry and voltage and current values to determine the electrical

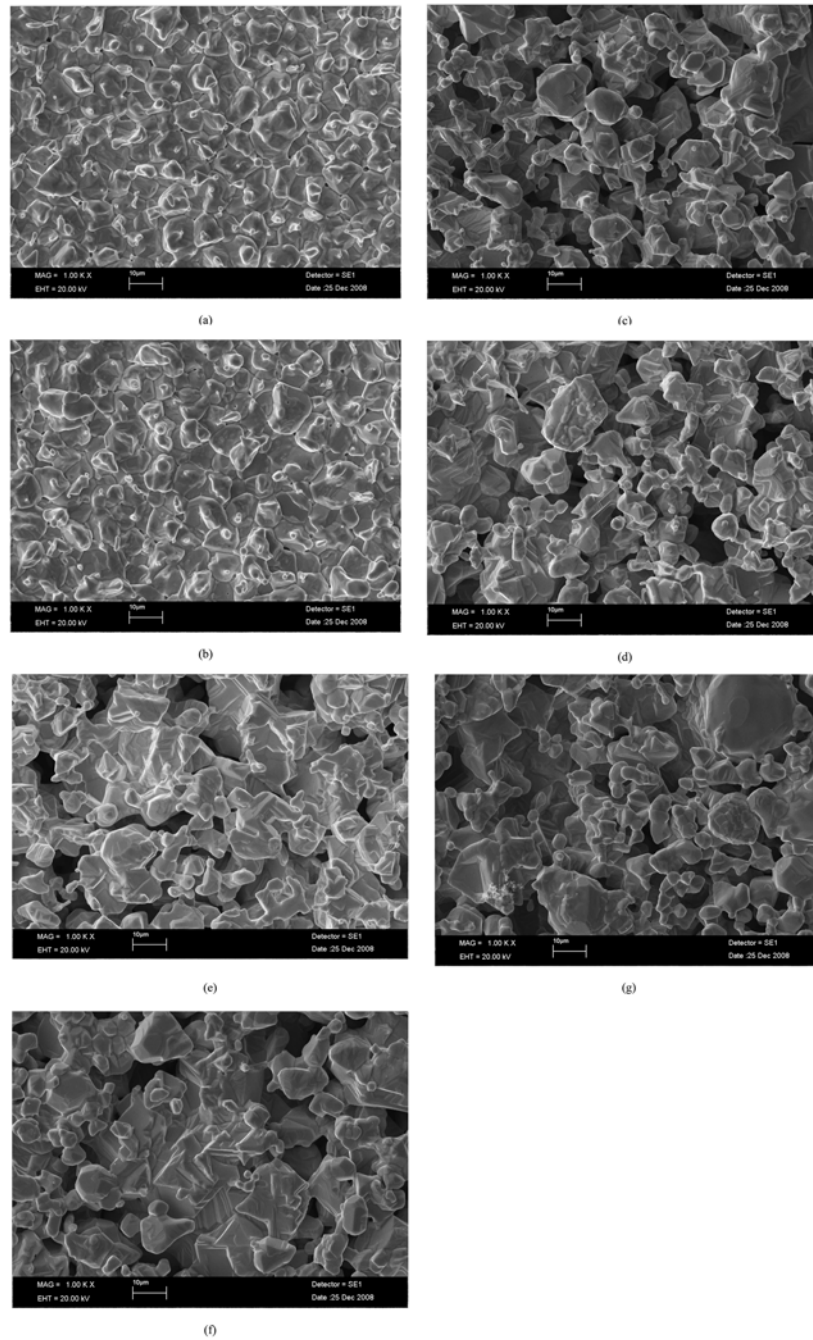


Fig. 4. SEM images of I- phase samples: (a) pure CdO (non-annealed) and (b) pure CdO (annealed at 850 °C), (c) 0.25, (d) 0.50, (e) 0.75, (f) 1, (g) 2 mol % Fe-doped CdO (after heating at 850 °C).

conductivity. In the calculation of resistivity a correction factor, which varies with the sample geometry and the positions of contacts on the sample, should be used along with the V and I values. According to the sample dimensions t/s 0,5 and $d/s < 40$ when these ratios are considered, in the light of previous studies, G is obtained as [25, 36, 37].

$$G = 2 \cdot \pi \cdot s \cdot F_1(t/s) \cdot F_2(d/s) \quad (2)$$

In this expression:

$$F_1(t/s) = \frac{t/s}{2.1n \left(\frac{\text{Sinh}(t/s)}{\text{Sinh}(t/2s)} \right)} = \frac{0.5}{2.1n \left(\frac{\text{Sinh}0,5}{\text{Sinh}0,25} \right)} = 0.345267 \quad (3)$$

$$F_2(d/s) = \frac{1n^2}{1n^2 + 1n \left(\frac{(d/s)^2 + 3}{(d/s)^2 - 3} \right)} = \frac{1n^2}{1n^2 + 1n \left(\frac{(6.5)^2 + 3}{(6.5)^2 - 3} \right)} = 0.829720 \quad (4)$$

where t is the thickness of the sample, d is the radius of

the sample, s is the distance between the probes, and F_1 and F_2 are additional correction factors. Finally, the G value is calculated as $0,3599 \text{ cm}$ [25, 36].

Both the values and the variation of the electrical conductivity of the pelleted powder CdO samples are in connected with their structure and changes. Further, the thermal treatments of the respective samples modify their structural characteristics and, consequently, their electrical properties. On this basis, the study of the temperature dependence of the electrical properties of CdO samples, may offer useful information about possible changes to the structure and characteristics of the CdO samples.

The temperature dependence of electrical conductivity (σ_{dc}) of the I-phase CdO pelleted powder samples after heating at 850°C were studied in the temperature range of $100\text{--}850^\circ\text{C}$. $\log(\sigma_T) \cdot 10^3/T$ graphs were drawn in order to show the conductivity change with respect to temperature. The graphs were compared with each other and the conductivity characteristics of the samples evaluated. The electrical conductivity plots versus temperature of undoped CdO and Fe-doped CdO I- phase samples (after heating at 850°C) are given in Fig. 5. As seen in the figure, the electrical conductivity of the I- phase samples increased with increase in temperature and show the semiconducting behaviour of pure and Fe-doped CdO samples. It is well known that the electrical conductivity of CdO samples is controlled by the intrinsic defects (oxygen vacancy and interstitial cadmium atoms) generated

at high temperature. We know that the electrical conductivity (σ) of CdO samples decreased with increased in temperature because the samples are semiconducting in nature [7].

Also, for CdO samples, increasing electrical conductivity with temperature can be explained by the following equations [38, 39].



After the ionization, the carrier concentration is increased by the two extra electrons. The electrical conductivity of the doped metal oxide semiconductors follows a mechanism in which the electron or hole hops from one localized site to the next. Whenever it is transferred to another site, the surrounding molecules respond to this perturbation with structural changes and the electron or hole is temporarily trapped in the potential well leading to atomic polarization. The electron resides at this site until it is thermally activated to migrate to another site. Another aspect of this charge hopping mechanism is that the electron or hole tends to associate with local defects [40]. Also, it must be stressed that the incorporation of iron to CdO leads to a slightly marked increase in electrical conductivity. This can be explained by considering the following: the electron concentration of the system increased with Fe content, originating from extra electrons generated to compensate for the electric charge balance by adding Fe^{3+} for Cd^{2+} , and the increased electron concentration gives rise to an increase in electrical conductivity. A similar condition was shown in other studies [16, 41]. The electrical conductivity value of the 1 mol % Fe-doped CdO sample (after heating at 850°C) at 100°C was 1349 , and at 850°C it was $2692 \Omega^{-1} \cdot \text{cm}^{-1}$. In another study, we observed that the electrical conductivity value of 1 mol % Cu-doped CdO sample (after heating at 850°C) at 100°C was 178 , and at 850°C it was $708 \Omega^{-1} \cdot \text{cm}^{-1}$. Namely, the effect of Fe doping on increasing the electrical conductivity of CdO samples is greater than Cu. We think that the substitution of Fe^{3+} for Cd^{2+} gives more electron than the substitution of Cu^{2+} or Cu^+ for Cd^{2+} and more electron concentration gives rise to a greater increase in electrical conductivity.

Conclusions

Fe-doped CdO powders were synthesized by using a solid state reaction method with metallic Fe powder and commercial pure CdO powder. The XRD analysis results indicated that all powder samples in the Fe-doped CdO binary system (0, 0.25, 0.50, 0.75, 1 and

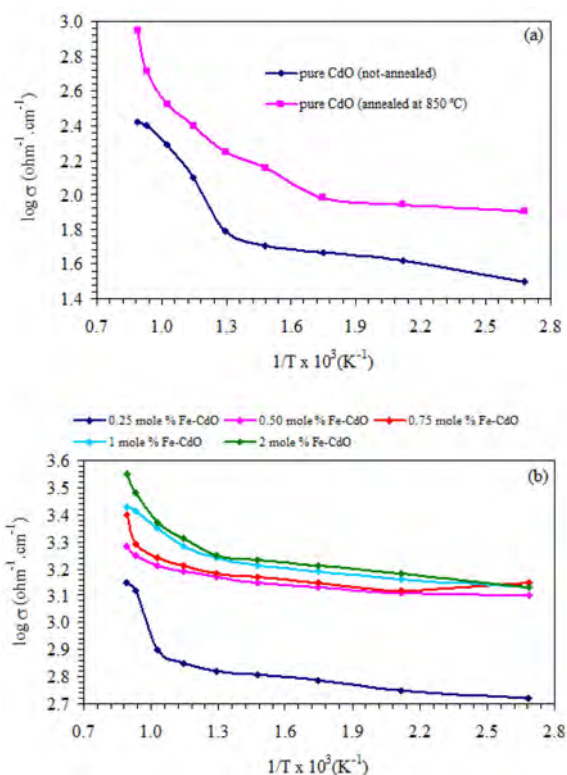


Fig. 5. Electrical conductivity plots for CdO samples: (a) undoped CdO, (b) Fe-doped CdO I- phase (after heating at 850°C).

2 mol %) had a cubic structure, namely the limit solubility of Fe ions in the CdO lattice at 850 °C. For pure and I- phase samples (after heating at 850 °C), the electrical conductivity increased with heat treatment and doping concentration. This can be explained by considering the following: the concentration of free electrons in the CdO sample increases with the increase in Fe doping concentrations because Fe has more valence electrons more than Cd.

Acknowledgments

This study was financially supported by the Research Foundation of Erciyes University (Kayseri, Turkey).

References

- P.K. Ghosh, S. Das, S. Kundoo and K.K. Chattopadhyay, *J. Sol-Gel Sci. Tech.* 34 (2005) 173-179.
- C.C. Vidyasagar, Y.A. Naik, T.G. Venkatesh and R. Viswanatha, *Powder Technol.* 214 (2011) 337-343.
- F.A. Benko, and F.P. Koffyberg, *Solid State Comm.* 57 (1986) 901-903.
- R.K. Gupta, K. Ghosh, R. Patel, S.R. Mishra and P.K. Kahol, *Mater. Lett.* 62 (2008) 3373-3375.
- Z. Zhao, D.L. Morel and C.S. Ferekides, *Thin Solid Films.* 413 (2002) 203-211.
- A. Shiori, *Jpn. Patent No:* 7 (1997) 909.
- C.H. Bhosale, A.V. Kambale, A.V. Kokate and K.Y. Rajpure, *Mat. Sci. Eng. B* 122 (2005) 67-71.
- O.A. Hamadi, N.J. Shakir and F.H. Mohammed, *Bulg. J. Phys.* 37 (2010) 223-231.
- C. Dantus, R.S. Rusu and G.I. Rusu, *Superlattice Microst.* 50 (2011) 303-310.
- R.S. Mane, H.M. Pahtan, C.D. Lokhande and S.H. Han, *Sol. Energy.* 80 (2006) 185-190.
- R.K. Gupta, K. Ghosh, R. Patel and P.K. Kahol, *J. Alloy. Compd.* 509 (2011) 4146-4149.
- A.A. Dakhel, *Sol. Energy.* 83 (2009) 934-939.
- A.A. Dakhel, *Sol. Energy.* 84 (2010) 1433-1438.
- B.J. Zheng, J.S. Lian, L. Zhao and Q. Jiang, *Appl. Surf. Sci.* 256 (2010) 2910-2914.
- R.K. Gupta, F. Yakuphanoglu and F.M. Amanullah, *Physica E* 43 (2011) 1666-1668.
- B.J. Zheng, J.S. Lian, L. Zhao and Q. Jiang, *Vacuum.* 85 (2011) 861-865.
- R. Kumaravel, K. Ramamurthi and V. Krishnakumar, *J. Phys. Chem. Solids.* 71 (2010) 1545-1549.
- R.J. Deokate, S.V. Salunkhe, G.L. Agawane, B.S. Pawar, S.M. Pawar, K.Y. Rajpure, A.V. Moholkar and J.H. Kim, *J. Alloy. Compd.* 496 (2010) 357-363.
- A.A. Dakhel, *Thin Solid Films.* 518 (2010) 1712-1715.
- L. Wang, Y. Pu, W. Fang, J. Dai, C. Zheng, C. Mo and C. Xiong, *Thin Solid Films.* 491 (2005) 323-327.
- U. De, M.K. Chattopadhyaya, S. Chaudhry and C. Sarkar, *J. Phys. Chem. Solid.* 61 (2000) 1955-1958.
- Inchem: Chemical Safety Information from Intergovernmental Organizations. <http://www.inchem.org/documents/icsc/icsc/eics0117.htm>. Retrieved on. (2007.2.16).
- J. Ostorero, A. Mauger, M. Guillot, A. Derory, M. Escorne and A. Morchand, *Phys. Rev. B* 40 (1989) 391-395.
- X. Mao, W. Zhong and Y. Du, *J. Magn. Magn. Mater.* 320 (2008) 1102-1105.
- S. Yilmaz, O. Turkoglu and I. Belenli, *Mater. Chem. Phys.* 112 (2008) 472-477.
- H. Colak and O. Turkoglu, *J. Mater. Sci: Mater. Electron.* 23 (2012) 1750-1758.
- Bruker AXS GmbH, *DiffraPlus PDF Maint Powder Diffraction Database Manager Software*, Printed in The Federal Republic of Germany (2000).
- Y. Yang, S. Jin, J. E. Medvedeva, J.R. Ireland, A.W. Metz, J. Ni, M.C. Hersam, A.J. Freeman, T.J. Marks, *J. American Chem. Soc.* 127 (2005) 8796-8804.
- A.J. Freeman, T.J. Marks, *J. American Chem. Soc.* 127 (2005) 8796-8804.
- B.J. Ingram, G.B. Gonzalez, D.R. Kammler, M.I. Bertoni, T.O. Mason, *J. Electroceram.* 13 (2004) 167-175.
- J.J. Kim, T.B. Hur, J.S. Kwak, D.Y. Kwon, Y.H. Hwang and H.K. Kim, *J. Korean Phys. Soc.* 47 (2005) 333-339.
- H. Colak and O. Turkoglu, *J. Mater. Sci. Technol.* 27 (2011) 944-950.
- H. Colak and O. Turkoglu, *J. Mater. Sci. Technol.* 28 (2012) 268-274.
- R.C. Weast, *Handbook of Chemistry and Physics*, 56nd ed. Crc Press (1975-1976).
- T.K. Subramanyam, S. Uthanna and B.S. Naidu, *Mater. Lett.* 35 (1998) 214-220.
- U. Ozgur, Y.I. Alivov, C. Liu, A. Teke, M.A. Reshchikov, S. Dogan, V. Avrutin, S.J. Cho and H. Morkoc, *J. Appl. Phys.* 98 (2005) 041301.
- S. Yilmaz, O. Turkoglu, and I. Belenli, *Ceramica.* 57 (2011) 185-192.
- D.K. Schroder, in *Semiconductor Material and Device Characterization*, John Wiley and Sons, USA (2008).
- J.A. Bastin and R.W. Wright, *Proc. Phys. Soc.* 72 (1958) 65-69.
- J.S. Chol, Y.H. Kang and K.H. Kim, *J. Phys. Chem.* 81 (1977) 2208-2211.
- M.S. Hossain, R. Islam and K.A. Khan, *Chalcogenide Letters.* 5 (2008) 1.
- B. Saha, R. Thopa and K.K. Chattopadhyay, *International Workshop on Physics of Semiconductor Devices 01/2008*. Doi: 10.1109/IWPSD.2007.4472539.